CCA-693

541.135.4:546.57.121
Conference Paper

Electrochemical Properties of Silver Halides and their Relation to Photography*

W. Jaenicke

Institute of Physical Chemistry, University of Erlangen-Nürnberg, Erlangen, Germany

Received January 20, 1972

A survey is given on the properties of AgCl, AgBr, and AgI as ionic conductors, as electronic conductors and as mixed conductors. The equilibria of disorder are discussed and the relaxation time of point imperfections is estimated. The electrochemical mechanism of dissolution and etching is outlined. The electronic equilibria and their dependence on the surroundings are described by the dependence between the Fermi energy and the halogen pressure or the silver activity. The mobilities of electrons and holes are discussed, especially the drift mobilities and the different kinds of traps in light of the formation kinetics of the latent image. Some reasons for the high sensitivity of silver halides are given.

Photographic development is a surface reaction catalyzed by a low overpotential at the latent image speck, not a redox process at a semiconductor electrode. Bleaching and latensification of inner latent images, however, can be explained by injection processes. The origin and sign of space charges in the surface region of the compounds, their experimental evidence and their influence on the electrochemical and photographic behaviour is considered. Some measurements of instationary polarization at silver halide—metal or —carbon contacts are described.

A) INTRODUCTION

The silver halides have scientific and technological importance because they exhibit a high ionic conductivity combined with an electronic conductivity which is low in darkness but which can be considerably enlarged by illumination.

It is this combination, which has made AgBr with some addition of AgI irreplaceable in high sensitive photography[1]. Nearly pure ionic conductivity at the other hand is found in silver iodide and some mixed salts like $RbAg_4I_5$. At room temperature the latter has the conductivity of concentrated fluid electrolytes[2] and may be of some interest as a solid electrolyte in power sources.

The electrochemistry of silver halides is closely connected with the above mentioned conductivity phenomena. This paper considers the properties which silver chloride, bromide, and iodide exhibit as salts, as semiconductors and

* Review paper presented as plenary lecture at the *22nd Meeting of the International Society of Electrochemistry*, Dubrovnik, Yugoslavia, September 1971.

in processes which are due to mixed conductivity such as latent images, redox processes, space charge layers and contact properties.

B) SILVER HALIDES AS SALTS

1. Ionic Disorder and Relaxation Time of Point Imperfections

Although silver halides have considerable covalent character, for most practical purposes they can be treated as ionic compounds. They are characterized by an almost ordered anion lattice, and a Frenkel disorder of the cations[3]. Some Schottky disorder is present[4] but it can be neglected at room temperature.

Part of the lattice sites can be occupied by foreign anions like S or cations like Cu, Cd. The rates ν_j, of exchange of places of the different point imperfections are of special importance with regard to the electrochemical properties. In Fig. 1 some values of ν_j are compiled as a function of temperature.

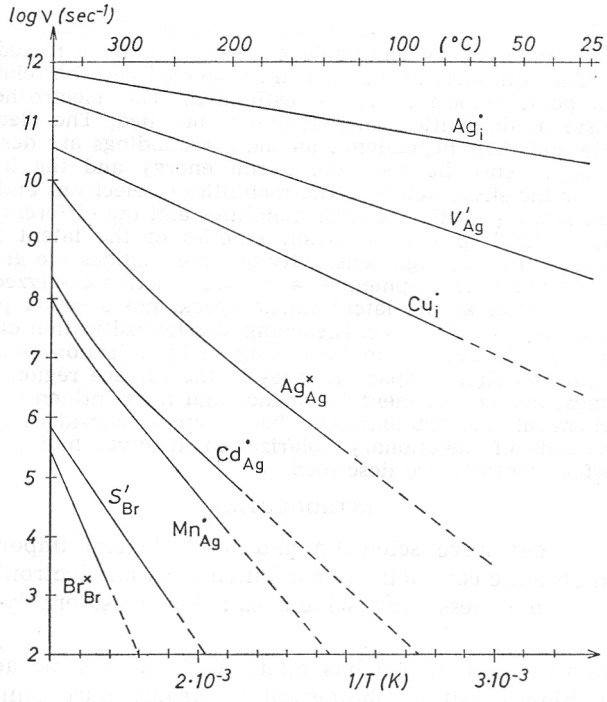

Fig. 1. Rate of exchange of places ν_j (sec^{-1}) in AgBr from conductivity ($Ag^{\cdot}_i$, V_{Ag}') and tracer diffusion experiments as a function of temperature (Calculated from[5]). Dashed: extrapolated values.

The diffusion coefficient of the imperfection D_j is connected with ν_j by the equation

$$D_j = \frac{RT}{z_j F}\, u_j \approx \frac{1}{6}\, \nu_j\, a^2 \qquad (1)$$

[u_j = electric mobility, z_j = charge number of the imperfection, a = jump distance (nearly equal to the distance between two lattice places)]. The

extrapolation at room temperature is rather uncertain, since most of the measurements were made at elevated temperatures. At room temperature any movement of anions can be neglected[31]. The diffusion rate of cations is slow compared with the diffusion rate of the Frenkel defects, especially, if the imperfections are charged. At room temperature the probability of the exchange of places of cation vacancies is about two orders of magnitude smaller than that of interstitials. [$u(Ag_i) = 5.3 \times 10^{-4}$ cm^2 V^{-1} s^{-1}; $u(V'_{Ag}) = 4.5 \times 10^{-6}$ cm^2 V^{-1} s^{-1}, ref. 64)]. This can be understood from Fig. 2[6].

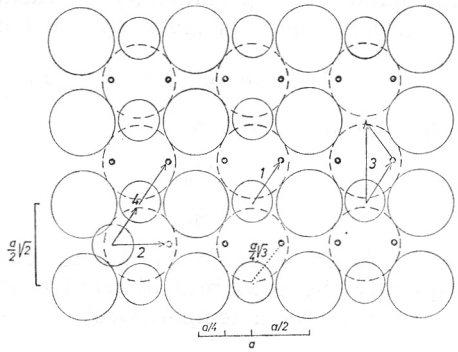

Fig. 2. Schematic view of an 110 plane of AgBr[6]. Large circles: Br^x_{Br}, small circles: Ag^x_{Ag}, dots: interstitial sites. *1:* Generation of a Frenkel defect, *2:* Interstitial diffusion, *3:* Vacancy diffusion, *4:* Interstitialcy diffusion. For clearness the radii of the spheres are 90% of the respective ionic radii.

For all cases in which the ionic equilibria within the crystals are considered it is required that the equilibria are established within a short time. Therefore it is necessary to know the relaxation time of the Frenkel equilibrium*

$$V_i^x + Ag_{Ag}^x \underset{k_{-1}}{\overset{k_1}{\rightleftarrows}} Ag_i^{\cdot} + V'_{Ag} \tag{2}$$

From this equilibrium it follows

$$\frac{-d[Ag_i^{\cdot}]}{dt} = k_{-1}[Ag_i^{\cdot}][V'_{Ag}] - k_1[V_i^x][Ag_{Ag}^x] \tag{3}$$

In pure crystals the concentrations of imperfections are equal. Therefore, with the deviation x from the equilibrium concentration of imperfections

$$x = [Ag_i^{\cdot}] - [\overline{Ag_i^{\cdot}}] \tag{4}$$

$$-\frac{dx}{dt} = k_{-1}([Ag_i^{\cdot}]^2 - [\overline{Ag_i^{\cdot}}]^2) \approx k_{-1} x \cdot 2[\overline{Ag_i^{\cdot}}] \tag{5}$$

By integration of eq. (5) the relaxation time τ is found:

$$\tau = \frac{1}{2k_{-1}[\overline{Ag_i^{\cdot}}]} \tag{6}$$

* The same nomenclature for the imperfections as Kröger[7] is used. V = vacancy. Superscripts $^{\cdot\,\prime\,x}$ = net charge + 1, —, 1, 0 of the defect. Subscript: Lattice site occupied by the defect (i = interstitial).

The reaction rate k_{-1} can be calculated, the reaction being diffusion controlled: Thus[8]:

$$k_{-1} = 4\pi [D(Ag_i^{\cdot}) + D(V'_{Ag})] \cdot N_L af^* \quad (7)$$

where $a \approx$ jump distance, f^* = factor which makes allowance for the Coulomb energy φ between the defects. For the mentioned case of attraction:

$$f^* \approx [\varphi(r = a)/kT] / [\exp \varphi(r = a)/kT - 1] = F^2/4\pi\varepsilon\varepsilon_0 N_L aRT \quad (8)$$

(ε = permittivity of the halide, ε_0 = permittivity of vacuum).

The sum of diffusion coefficients is given by the ionic conductivity $\varkappa_{ion}$:

$$\varkappa_{ion} = F[\overline{Ag}_i^{\cdot}]\{u(Ag_i^{\cdot}) + u(V'_{Ag})\} \quad (9)$$

From (1), (6), (7), (8), (9) the relaxation time is

$$\tau = \frac{\varepsilon\varepsilon_0}{2\varkappa_{ion}}$$

At room temperature $\varkappa_{ion}$ (AgBr) is about $3 \times 10^{-8}\ \Omega^{-1}\ cm^{-1}$ (ref. 64) therefore $\tau \approx 2 \cdot 10^{-5}$ sec. Consequently the equilibria of point defects in silver halides are established quickly even at room temperature[63].

2. Electrochemical Theory of Dissolution and Etching of Salts like Silver Halides

A simple theory of the dissolution of silver halides[9] was derived by means of the assumption, that the exchange rate of anions and cations between crystal surface and solution is different and dependent on concentration and potential. In the case of equilibrium the current-potential curves intersect at zero current. During dissolution at open circuit an overpotential is established, which guarantees equal net currents of anions and cations. As an example Fig. 3a shows the concentration profile within the diffusion layer during the complex dissolution of silver chloride by thiosulfate. If the rate of stirring is enlarged, the thickness of the diffusion layer changes from δ to δ'. The concentration of the halide ions (X) at the phase boundary remains nearly constant. Therefore the current-potential curve of the anion transfer is not changed (Fig. 3a). The same is valid for the cathodic portion of the current-potential curve of the cations *i. e.* for the dissociation of the complex MY_n. However, to form the complex at a higher rate, the surface concentration of the solvent Y has to increase considerably with increasing rate of stirring. This is possible without measurable change of the diffusion conditions (Fig. 3b). Therefore the anodic portion of the current-potential curve of the cations is shifted. In this way if the reaction rate increases (Fig. 3a) the total current-potential curve of the cation becomes steeper, and the point of intersection with the curve of the anions which gives the reaction current, is shifted to more negative potentials.

This theory was verified for anodic layers of silver halides (Fig. 4). It is only valid for strongly disturbed crystal surfaces[44]. At single crystals the separation of ions from the surface should be a two-step process, the rate determining step being the leaving of an ion from a growth site. The stationary number of cathodic and anodic growth sites is regulated by the respective potentials which depend upon the activation energies of separation[10]. New experiments

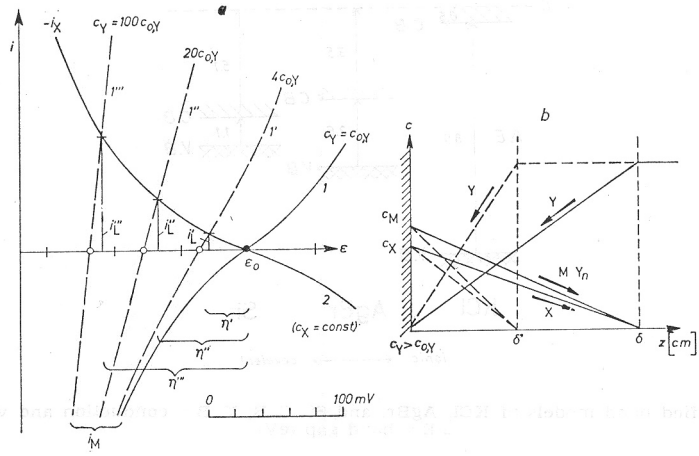

Fig. 3. Dissolution of salts in complexing agents[9].

a) Current -potential curves. 1: complex dissolution and deposition of the cation M at equilibrium; 1', 1'', and 1''' like 1 at increasing dissolution rates; 2: dissolution and deposition of anion X. i', i'', and i''' are net dissolution rates. η', η'', and η''' are overpotentials.

b) Concentration profile at the surface of the salts in stirred solutions. — concentrations at low dissolution rate (thickness of the double layer = δ). — — — concentrations at high dissolution rate (thickness of diffusion layer = δ').

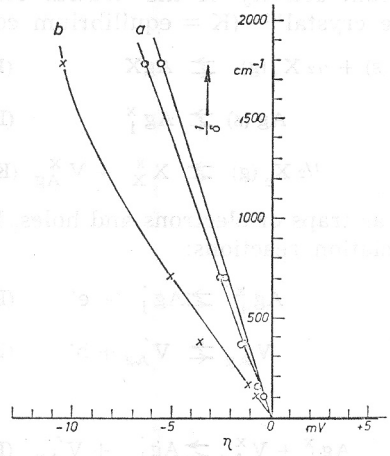

Fig. 4. Overpotentials η during the complex dissolution of silver halides as a function of the dissolution rate, measured as reciprocal diffusion layer thickness δ^{-1}. Dissolution of *a)* AgBr in $S_2O_3^{2-}$; *b)* AgCl in $S_2O_3^{2-}$.

with single crystals of salts making use of this refinement of the theory were performed by Ibl[11].

C) ELECTRONIC CONDUCTIVITY OF SILVER HALIDES

1. The Complete Equilibria in Silver Halides

Silver halides likewise show some electronic dark conductivity. As is seen from the simplified band models of Fig. 5 they occupy a middle position between covalent compounds like silicon and ionic compounds like the alkali halides.

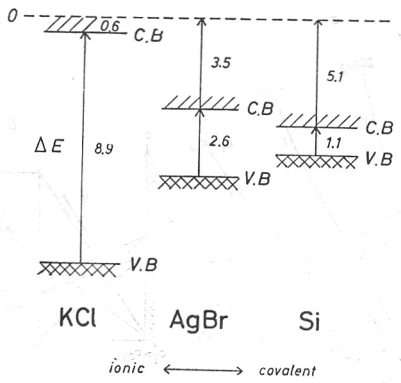

Fig. 5. Simplified band models of KCl, AgBr, and Si. C. B, V. B = conduction and valence band. ΔE = band gap (eV).

In contrast to the latter, photoexcitation of electrons in silver halides is always combined with photocurrents[12].

The dark conductivity is determined by the redox potential of the adjacent phase. Corresponding to the activity of the silver and the halide in the surroundings, an equilibrium activity of the neutral components is established within the bulk of the crystal[4,13] (K = equilibrium constants):

$$Ag\,(s) + {}^1/_2\,X_2\,(g) \rightleftarrows AgX \qquad (K_0) \tag{10}$$

$$Ag\,(s) \rightleftarrows Ag_i^x \qquad (K_M) \tag{11}$$

$${}^1/_2\,X_2\,(g) \rightleftarrows X_X^x + V_{Ag}^x \qquad (K_X) \tag{12}$$

The atomic defects act as traps of electrons and holes. Free carriers are formed according to the dissociation reactions:

$$Ag_i^x \rightleftarrows Ag_i^{\cdot} + e' \qquad (K_e) \tag{13}$$

$$V_{Ag}^x \rightleftarrows V'_{Ag} + h^{\cdot} \qquad (K_h) \tag{14}$$

or:

$$Ag_i^x + V_{Ag}^x \rightleftarrows Ag_i^{\cdot} + V'_{Ag} \qquad (K'_F) \tag{15}$$

If the Frenkel equilibrium

$$0 \rightleftarrows Ag_i^{\cdot} + V'_{Ag} \qquad (K_F) \tag{16}$$

(cf. eq. (2)) is also considered, one obtains from eq. (13)—(16) the electronic equilibrium

$$0 \rightleftarrows h^{\cdot} + e' \qquad (K_i) \tag{17}$$

There is only a small deviation from the stoichiometry, but the equilibria can be adjusted at room temperature. Therefore, ionic and electronic processes in silver halides always are coupled, in contrast to semiconductors, such as silicon, which are of technical interest, because the ionic processes are frozen in.

If the condition of electroneutrality in the bulk of the crystal is included, all concentrations can be calculated and plotted as a function of halogen or silver activity. This is shown in Fig. 6[14] for pure AgBr (for which $K_F \gg K_i$).

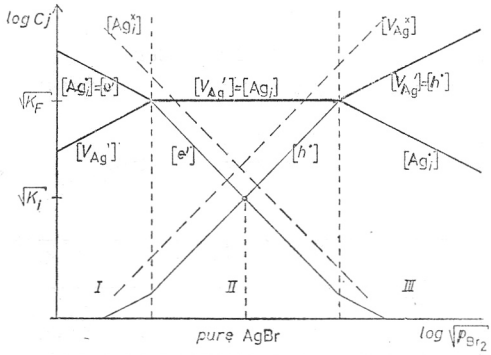

Fig. 6. Concentrations (ordinate) of imperfections in pure AgBr as a function of bromine activity (abscissa)[14]. I: region of electron conductivity ([Ag$_i^{\cdot}$] = [e$^{\prime}$]); II: region of ionic conductivity ([Ag$_i^{\cdot}$] = [V$^{\prime}_{Ag}$]); III: region of hole conductivity ([V$^{\prime}_{Ag}$] = [h$^{\cdot}$]); dashed lines: concentration of filled traps.

Similarly more complicated cases can be treated[7], *e. g.* the addition of foreign ions of higher valence (M^{2+}). In this case *n*-type conductivity rises[15]: If $[M^{2+}] > K_F^{1/2}$:

$$\log n = \log n_0 + \log \frac{[M^{2+}]}{K_F^{1/2}} \tag{18}$$

(n, n_0 = electron concentrations in doped and pure crystals). The association of ionic defects can be measured by means of glow curves (ionic thermocurrents)[60]. At low temperatures imperfections at structural defects or dislocations become predominant.

2. The Regulation of the Fermi Energy

The dependence of electron and hole concentrations on the halogen activity is equivalent to the statement that the Fermi energy is adjusted between certain limits by the redox potential of the surroundings[16]. The Fermi energy E_F can be written as

$$E_F = -\frac{E_i}{2} + \frac{kT}{2} \ln K_i - kT \ln p \tag{19}$$

(E_i = band gap, p = concentration of holes). Therefore it follows from eqs. (12) and (14) that

$$E_F = \text{const} - kT \ln [X_2]^{1/2} \tag{20}$$

For AgBr at 300° K this is shown in Fig. 7. It follows that great *p*-type conductivity but only small *n*-type conductivity can be achieved. The latter is increased by addition of divalent cations (dashed line). In the figure the limits bromine pressure = 1 atm and activity of silver = 1 ($P_{Br_2} = 10^{-16.8}$ atm) are inserted.

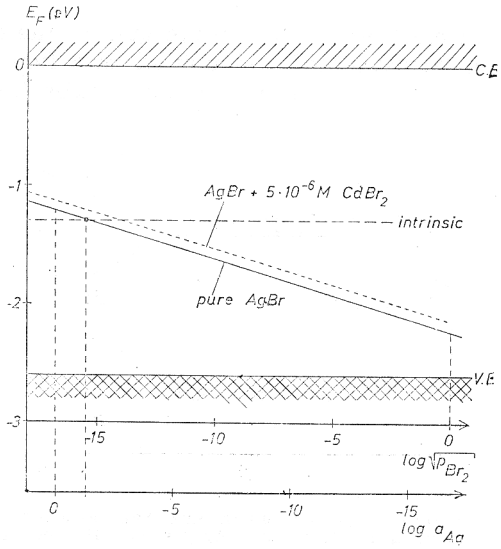

Fig. 7. Fermi energy E_1 (eV) of pure doped AgBr as a function of a_{Ag} or P_{Br_2} (atm) at 300 K.

3. *The Direct Measurement of Electronic Disorder*

The direct measurement of the small deviation of stoichiometry is possible by an electrochemical trick, due to Hebb and Wagner[17]. They first used a stationary polarization of galvanic cells with a silver halide as an electrolyte between a reversible halogen or silver electrode and a second electrode, which blocked the ionic part of the current.

Fig. 8 illustrates recent results for silver chloride[18]. If in the left cell the right, blocking electrode is made cathodic, the first effect is migration of holes and silver ions. However, below the decomposition potential, a steady state concentration gradient of interstitial silver ions is built up near the cathode, which counteracts the potential gradient. Therefore in the bulk no electric field remains. The holes are transported only by diffusion, a linear gradient

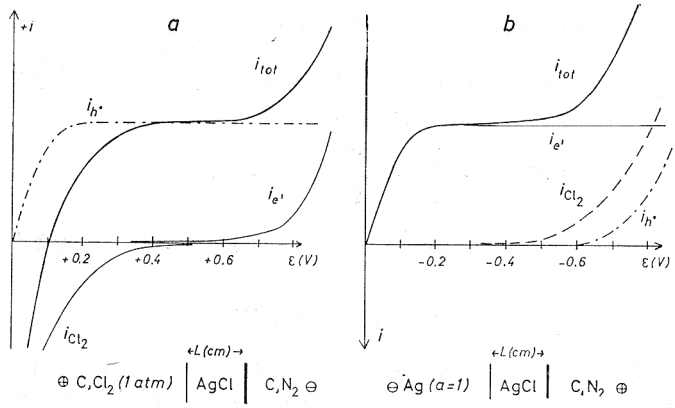

Fig. 3. Stationary currents of electronic carriers during the polarisation of cells with a reversible electrode and an inert electronically conducting electrode[18].

being established through the whole crystal of thickness L. ($L \gg d$, d being the thickness of the space charge layers at the phase boundaries).

With increasing cathodic polarisation the current rises up to a limiting current. At still higher potentials, the silver activity at the cathode increases so much, that electrons are generated, which cause a diffusion current of opposite direction and of exponential shape. Some leakage current cannot be prevented.

In the right cell (Fig. 8b) the blocking electrode on the right must be polarized anodically. At low potentials electrons are generated and are able to diffuse, while a concentration gradient of silver vacancies is built up at the anode. The electronic portion of the stationary current in the cell is given by

$$i_e + i_h = \frac{RT}{FL} [\varkappa_h (1 - \exp(-\varepsilon F/RT)] + \varkappa_e [\exp(\varepsilon F/RT) - 1] \tag{21}$$

The conductivities $\varkappa$ measured in both cells I and II are connected by the free enthalpy ΔG of silver halide formation [eq. (10), *e. g.* for the holes:

$$\frac{\varkappa_h \, I}{\varkappa_h \, II} = \frac{[h_I^{\cdot}]}{[h_{II}^{\cdot}]} = \frac{P_{Cl_2}(I)^{1/2}}{P_{Cl_2}(II)^{1/2}} = \frac{1}{P_{Cl_2}(II)^{1/2}} \tag{22}$$

$$P_{Cl_2}(II)^{1/2} \cdot a_{Ag}(II) = P_{Cl_2}(II)^{1/2} = \exp(-\Delta G/RT) \tag{23}$$

4. Mobilities, Mobile and Trapped Electronic Charge Carriers

The knowledge of trapping processes and of mobilities is not only necessary to calculate concentrations from conductivities, but also to understand the photographic processes.

There are several methods, but they measure different mobilities: Free carriers are studied by means of the Hall effect. The Hall mobility of holes u_h can easily be measured if the halide is in contact with halogen[19]. The Hall mobility of electrons u_e can only be measured with photoexcited electrons[20]. In the latter case the hole mobilities can be neglected since $u_h \ll u_e$. At room temperature $u_e \approx 70$ cm²/Vsec, $u_h \approx 2$ cm²/Vsec.

A drift mobility is found from the displacement of photoelectrons and holes by field pulses[21]. The same method can be used to measure life times, if a time lag is used between light and field pulses[22]. The measured drift mobilities depend on crystal preparation and deformation. Shallow electron traps ($\geqq 0.05$ eV) have been observed, while the hole traps in general are deeper ($\geqq 0.4$ eV) Such hole traps preferentially are point defects like copper or sulfur ions[23].

Entirely different results are obtained, if the carriers migrate into a crystal by diffusion[24] or in form of a moving boundary*. Under these conditions all deep traps are filled during the migration. Migration of holes is obtained,

* A diffusion method for the drift mobility of electrons by means of the polarization decay in the galvanic cell Ag | AgBr | C was proposed by Weiss[61], however there are difficulties of interpretation owing to the double layer capacity (see **Chapter D 4)**[62].

if a silver bromide crystal is polarized between a bromide and a bromine solution in the following cell[25]:

$$Pt \mid Br_2,\ Br^- \mid AgBr \mid Br^- \mid Ag$$

If the electronic conductivity is comparable with the ionic conductivity, the moving of the boundary during a galvanostatic run can be measured by the potential difference along the crystal as a function of time. The resulting mobility is given in Fig. 9 as a function of temperature. At room temperature it is only a small fraction of the Hall mobility, the ratio being equal to the ratio

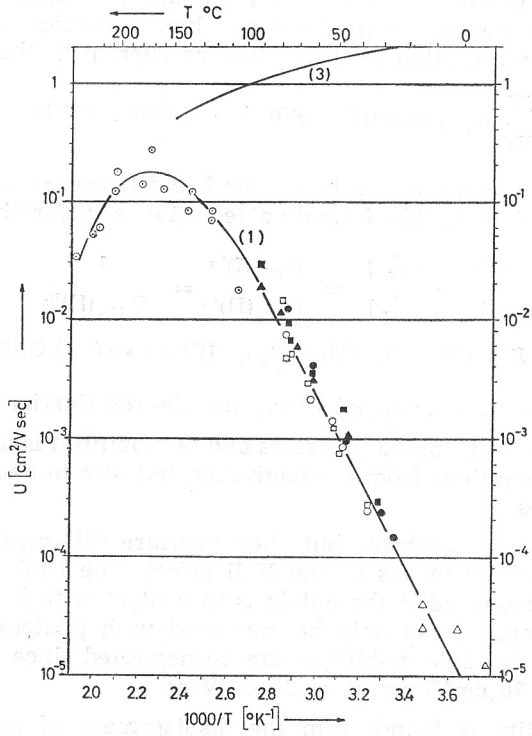

Fig. 9. Logarithm of hole mobilities in AgBr as a function of reciprocal temperature[25]. Curve (1) drift mobility □ ○ △ ■ ● ▲ measured with moving boundary. Q Q measured with diffusion. Curve (3): Hall mobility according to[19].

of free to total carriers. The ratio increases with temperature, corresponding to the dissociation of the traps, until it becomes equal to the Hall mobility. The depth of the traps is 0.78 eV. Still deeper traps are observed in deformed crystals. At the surface of pure silver halides the life time of holes is much larger than in the bulk[23].

Deep surface traps are of special importance for the primary photographic processes. They can be produced by cautious reduction of the halides, in presence of sulfur or gold compounds, as is done by the so called chemical ripening of photographic emulsions. It seems that the surface traps of positive net charge preferentially act as electron traps, whereas the uncharged act as hole traps. The state of surface traps depends on the crystal plane at wich they are deposited[26].

D) REACTIONS BETWEEN IONIC AND ELECTRONIC DEFECTS IN SILVER HALIDES

1. The Latent Image

The primary processes of photography are closely connected with the electronic, ionic and structural imperfections and their mobilities and life times. An immense quantity of experimental data collected during the last fifty years has shown[1] that the latent image is composed of only a few silver atoms and electrons which are condensed by alternating ion and electron trapping. Recently it has become possible to simulate quantitatively the formation kinetics of the latent image by the Monte Carlo method[27] or by solving the system of differential equations by an analog computer[28]. Fig. 10 shows the scheme,

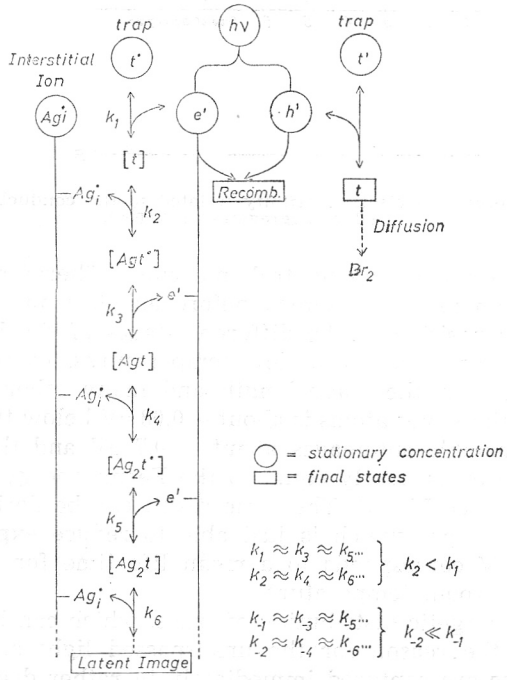

Fig. 10. Scheme of the latent image formation kinetics after the statistical theory of Hamilton and Bayer[27]. (In deviation of[27] positively charged traps as intermediates are assumed).

which was used in the first mentioned method. Irradiance and electron concentration were assumed as stationary, and the reservoir of silver ions and traps as large. All growth processes of the nucleus are of the second order, and all decomposition reactions are of the first order. The results can be used to explain the observed reciprocity failure and other instationarity phenomena.

In this calculation no energetic differences were assumed between nuclei of different sizes. Actually the energy is lowered during the growth. An original attempt to obtain a chemical picture of the nucleus recently was made by Trautweiler[29] (Fig. 11). He roughly estimated the bond energies of silver molecules and molecular ions (Ag_2^+, Ag_2, Ag_3^+ *etc.*) in silver bromide. It was concluded that in the dielectric medium negatively charged small molecular ions were unstable and that the positively charged molecular ions were more

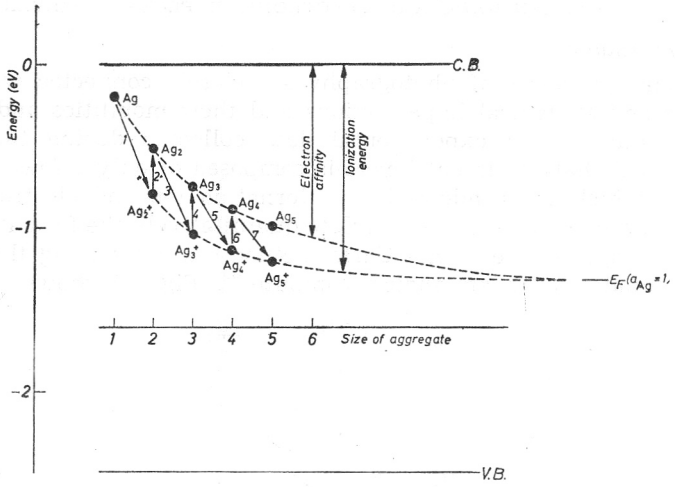

Fig. 11. Ionization energy and electron affinity (related to the conduction band C. B) of small silver aggregates in AgBr[29].

stable than the corresponding neutral molecules. Therefore during the latent image formation an ion is consumed before an electron is trapped. (Fig. 11.)

The energetic position of the different stages of the latent image can be derived from the luminescence at low temperatures, from the dependence of the Herschel effect on the wave length and many other observations[30]. The energy of interstitial silver atoms is about —0.03 eV below the conduction band.[4] The energy of unstable subimages about — 0.7 eV and that of stable images —1.2 eV. The energy is nearly equal to the Fermi energy of silver in contact with silver halide (see Fig. 7). The same result can be derived from the redox potential of a developer which is just able to reduce exposed crystals[32]. The energy of —1.2 eV corresponds to a mean life time for the latent image of about 10 years at room temperature.

The special energetic distribution of traps, which can be achieved in silver halides, may be the reason for the unsurpassed light sensitivity of AgBr[33]: photoexcited holes are captured immediately in rather deep traps, where they associate vacancies and are able to diffuse as uncharged particles. The electrons in the interior of the crystals can be captured many times in shallow traps (*e. g.* $Ag_i^{\cdot}$ at dislocations) until they reach deep traps, which are only available at the surface of chemically sensitized crystals. In this way it is possible that all photoelectrons are collected in few nuclei at the crystal surface where development is possible.

2. *Reduction and Oxidation Processes at Silver Halides (Bleaching and Development)*

The latent image formation is a light-induced redox process. It is obvious to assume the same mechanism to be valid for the following chemical redox process, the development. The system silver halide — developer may be treated as a semiconductor electrode with electron injection from the developer into the crystal and reaction of electrons and silver ions at the nucleus[34]. The

reverse process, the bleaching of the latent image, could be performed by hole injection.

This treatment, however, is unsuitable. The injection rate is much too small to explain the observed rate of development. This can be shown, if the mentioned relation between Fermi energy (redox potential) and concentration of electronic defects is used (see Chapter C3)[35]. The nuclei of the latent image can grow by silver halide reduction, if the redox potential of the developer is more negative than the potential of the latent image in contact with the crystal. The minimum value of this potential is that of metallic silver. To avoid spontaneous nucleation of silver at the unexposed crystals the developer potential should not be lower than 0.3 V below the silver potential[36]. A developer solution of this potential (Fig. 12.) is in equilibrium with an n-type silver

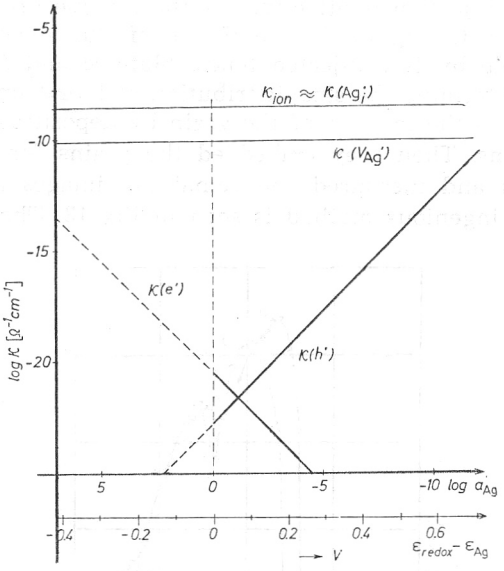

Fig. 12. Isotherms for the conductivities $\varkappa$ of different imperfections in pure AgBr at 25° C as a function of silver activity and redox potentials (calculated from[4]). dashed: area of metastability ($a_{Ag} > 1$).

bromide of an electron conductivity $\varkappa_e$ of about 4×10^{-15} Ω^{-1} cm^{-1} (25° C). The maximum rate development is given by the diffusion rate of electrons to a nucleus within the crystal, the diffusion rate of interstitial silver ions being greater than that of electrons ($\varkappa_{ion}/\varkappa_e \approx 10^5$). Using the boundary conditions of diffusion controlled reactions[8] (the nucleus being immobile, see equation (7)) the diffusion rate immediately becomes stationary. If r is the radius of the nucleus, the diffusion current j is given by

$$j = \frac{RT}{F^2} \cdot 4\pi\varkappa_e \cdot r \tag{24}$$

or integrated (v: molar volume of silver):

$$\left(\frac{r}{r_0}\right)^2 = 1 + \frac{2\,vRT\,\varkappa_e\,t}{F^2 r_0^2} \tag{25}$$

From eq (25) it can be calculated that a nucleus of an initial diameter 2 $r_0 = 6$ Å grows within 10 minutes to about 6.04 Å. Better results may be obtained if there are space charges of the right sign at the crystal surface (see Chapter D 3). But even with a surface potential which is 0.3 V more positive than the bulk potential, the nucleus reaches a diameter of not more than 66 Å within 10 min ($\varkappa_e$ at the surface $= 4 \times 10^{-11}\ \Omega^{-1}\ cm^{-1}$). Therefore intensification of a latent image by means of electron injection into the crystal is possible[50], but development can be excluded. Only surface latent images which are in contact with the developer grow corresponding to a local cell mechanism[37]. Since the reaction area grows strongly during the first stages of development, autocatalysis is observed. Inner latent images can be reduced only if the crystal is dissolved by complexation during the development.

However, hole injection is effective for the reverse process, the bleaching of the latent image. Owing to the small size of the nucleus a rather quick oxidation is possible by few injected holes. Matejec and Moisar[38] have used hole injection to determine the size distribution of latent images. They shifted the latent image into the interior of the grain by depositing new silver halide upon exposed grains. Then they embedded the grains for different times in oxidizing solutions and measured the remaining images after development. The result of this ingenious method is seen in Fig 13. The maximum of this

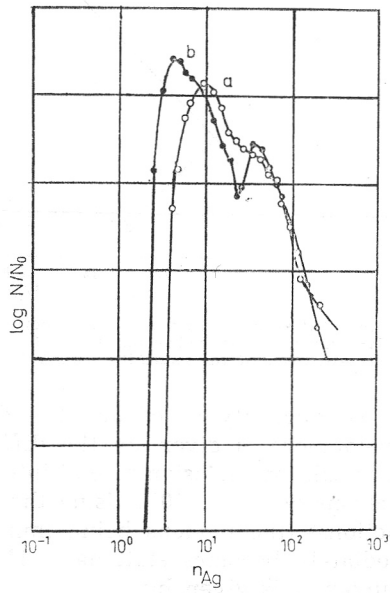

Fig. 13. Size distribution of (surface) latent images, as found by the method of Matejec and Moisar[38]. Abscissa: number of silver atoms per nucleus; ordinate: relative number of nuclei (logarithmic).
a) high intensity exposure; *b)* low intensity exposure.

size distribution curve confirms that latent images consist of about 10 Ag-atoms. Characteristic differences between high and low intensity exposure were observed.

3. Space Charge Layers and Surfaces

Thus far, only the bulk properties of the silver halides have been considered. The surface also needs a special consideration. Surface states exist also in pure crystals. A calculation using electron affinity, ionisation potential and Madelung energy shows that the surface states in pure silver halides are situated close to the edges of the conduction and the valence bands[39]. Therefore they could not be observed spectroscopically[40]. The latent images, however, may be regarded as surface levels not far from the middle of the band gap[29, 41].

The potential at the crystal surface is mainly influenced by ionic defects which are distributed unsymmetrically in the subsurface region. If the free enthalpies to form a vacancy and to form an interstitial site are different, electroneutrality cannot be maintained at the surface[42]. For calculational purposes the production of a Frenkel defect is divided into the transfer of a cation from a lattice position to a growth site at the surface and from the growth site to an interstitial position. In general both processes require different free enthalpies. In this way cations are enriched at the surface, and a positive surface potential φ results, if the free enthalpy of formation of the interstitials, ΔG_i, is greater than that of the vacancies ΔG_v

$$\varphi = \frac{\Delta G_i - \Delta G_v}{2F} \approx \frac{\Delta H_i - \Delta H_v}{2F} \tag{26}$$

In contact with a solvent the solvatation energy must also be considered. Since the free enthalpy of solvatation of the cations exceeds that of the anions, a negative surface charge is formed in contact with the pure solvent which must be compensated by a positive space charge within the solution. In the system, crystal — solution, the surface charges disappear and only two space charges of different sign remain, if the surface has no special properties. A theory for this case was developed by Grimley and Mott[43]. There are conditions, however, where the surface charges play a role[44]. In this case two space charges of equal sign can be separated by a surface charge of opposite sign.

In all cases the potential φ as a function of distance x from the surface can be derived according to the Gouy-Chapman theory from the Poisson-Boltzmann equations[45]. Under these conditions, the ionic and electronic equilibria are maintained in the space charge region. It follows that in a region which has an excess of interstitial cations (positive space charge) holes are enriched and *p*-type conductivity is found, and *vice versa*. On account of the small concentration of electronic carriers, only the ions need to be considered in the calculation of the potential.

There must be a considerable influence of space charges upon the processes in silver halides. The subsurface field is able to separate photogenerated electron-hole pairs[59] and to prevent recombination reactions[46]. According to its sign the diffusion potential may promote or block the injection of electrons into the crystal from a developer (see chapter D 2) or from an adsorbed optical sensitizer.

In spite of the importance of these effects there is lack of experimental data. There are many papers about the phase boundary, silver halide — solution or — vacuum problems. Calculations of space charges from thermodynamic and lattice parameters[47], measurements of surface resistances at right angle[48] or

in parallel[49] to the phase boundary, measurements of contact and ζ-potentials[44,51] or capacities[52], have been attempted but the results disagree. Experiments of Sounders, Tyler and West[52] are rather convincing. They exposed silver bromide single crystals by a light flash in coincidence with a pulsed electric field, which displaced photoelectrons against the back side of the crystals. The distribution of latent images which were formed by the photoelectrons in the subsurface region of the crystal could be measured when the back side of the crystal was etched in form of a wedge before development (Fig. 14).

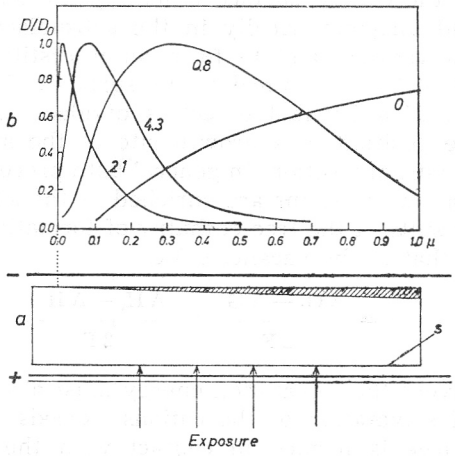

Fig. 14) a) Vertical section of AgBr single crystals as used for the experiments of Saunders, Tyler and West[52]. Large surface = (200). Exposure from below.
Field between transparent conducting glass (positive) and metal plate (negative). s = crystal surface covered with Ag_2S as hole trapping substance. Hatched: cross section, etched after illumination, before development.
b) relative distribution of images in the subsurface region of the crystal (Fig. 14 a) as a function of distance from the back side. Parameter: Field strength (kV/cm).

A maximum density of latent images was found below the surface. It was shifted with increasing field strength towards the back side. This could be explained by a counter field in the subsurface region. At the place, where the fields are balanced one has the greatest concentration of photoelectrons and the highest density of the latent images.

The calculated distribution of latent images from the Gouy-Chapman theory is in exact agreement with the experiments[53]. A surface potential of about —0.15 V was found. The negative surface charge was compensated by a positive space charge of interstitial silver ions. Consequently the free energy of formation of vacancies should be greater than that of interstitials. This, however, is in contradiction to calculations and other measurements[42,47] (Fig. 15).

Fig. 16 shows the two possibilities for describing the spatial dependence of the potential. A surprising result favours Sounders' view: In his experiments the distribution of latent images within the crystals remained nearly unchanged if the back side of the crystal was dipped either in potassium bromide or in silver nitrate solutions during the exposure. This means that there is only a small influence of the ζ-potential upon the space charge within the crystal. Further experimentation is necessary. Perhaps there are differences between crystals, grown from the melt and grown from the solution.

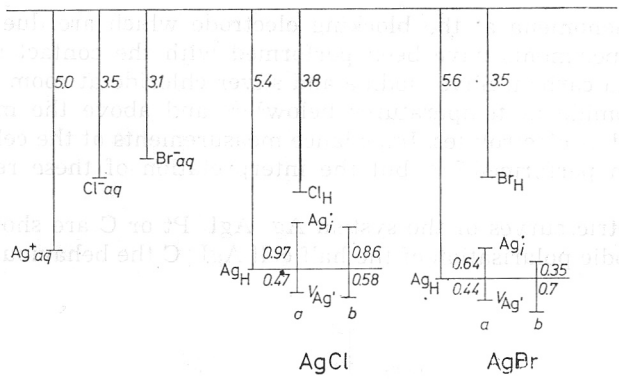

Fig. 15. Energies (eV) of lattice particles in AgBr and AgCl and of ions in aqueous solution. (Calculated from lattice energies and single ion solvatation energies, under the assumption that the total heats of solution and of solvatation can be divided into values of single ions in the same ratio. Index H = growth site. Frenkel energies of AgCl: *a)* after Kliewer[42]; *b)* after Sliwkin[42]. Frenkel energies of AgBr: *a)* after Matejec[47]; *b)* after Trautweiler[53].

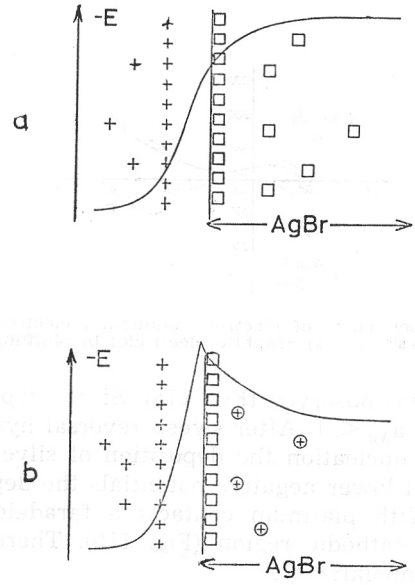

Fig. 16. Space charges and surface charges at the phase boundary AgBr/solution in the case of a negatively charged crystal surface. Ordinate = potential. a) after Matejec and Meyer[47], Grimley and Mott[48]; b) after Saunders[52], Trautweiler[53].

□ = v'_{Ag} ○ = Ag_i + = excess cations in the solution.

4. *Instationary Measurements at the Surface Silver Halide/Metal or Carbon*

As it was outlined in Chapter C 2, galvanic cells with a reversible and a blocking electrode such as Ag | AgCl | C or C, Cl_2 | AgCl | C are suitable to measure electronic conductivities in the electrolyte if they are stationary polarized. With the same systems under instationary conditions there are interesting

capacitance phenomena at the blocking electrode which are due to ionic processes. The experiments have been performed with the contact materials platinum, gold and carbon. Silver iodide and silver chloride at room temperature[54] and silver bromide at temperatures below[51,55] and above the melting point[56] have been used as electrolytes. Impedance measurements at the cell Ag|AgBr|Ag have also been performed[57,58], but the interpretation of these results is more difficult.

Voltammetric curves of the system Ag | AgI | Pt or C are shown in Fig. 17. During a cathodic polarisation of the half cell AgI | C the behaviour of an ideally

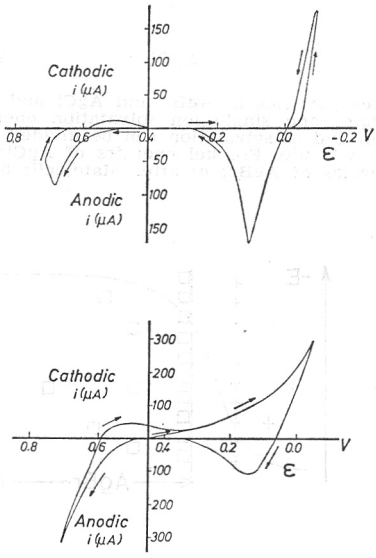

Fig. 17. Current potential behaviour of electron conducting electrodes in contact with AgI[54]. Sweep rate: 0,005 Vs^{-1} a) graphite electrode; b) platinum electrode.

polarisable electrode was observed (Fig. 17a). Silver deposition is not possible at potentials for which $a_{Ag} < 1$. After sweep reversal hysteresis is found, since after the beginning of nucleation the deposition of silver can be continued at lower activities. At still lower negative potentials the deposited silver becomes oxidized anodically. With platinum contacts a faradaic current is observed throughout the entire cathodic region (Fig. 17b). Therefore cathodically the electrode AgI | Pt is unpolarizable.

These observations are confirmed by potentiostatic measurements with pulses of 5 mV. At a silver iodide-graphite contact in the potential region —0.03 up to +0.5 V the current decays like the discharge of a condenser of 8 μF/cm^2. There is no silver deposition. The observed capacity corresponds to a plate condenser, composed of silver ions in the iodide and electrons in the graphite at closest distance (permittivity $\varepsilon = 1$). At the platinum contacts during a potentiostatic pulse the equilibrium is readjusted immediately, a submonolayer of silver being formed on the platinum. This corresponds to apparent capacities of about 10 000 μF/cm^2 during a potential step. A minimum value of the capacity is found at flat band conditions ($a_{Ag} = a_I$). If the measurement is per-

formed within the microsecond region, the apparent capacity diminishes. True capacity measurements therefore require nanosecond techniques.

Similar results are obtained with silver bromide as an electrolyte[55], but the discussion is more complicated because there is a greater extension of the space charges into the bulk of the crystal. In this system frequency dispersion was found.

Galvanostatic experiments of silver halide-carbon contacts are useful to examine nucleation phenomena in silver halide systems. As it is shown in Fig. 18, nucleation is accompanied with crystallisation overpotentials[54,55]. The

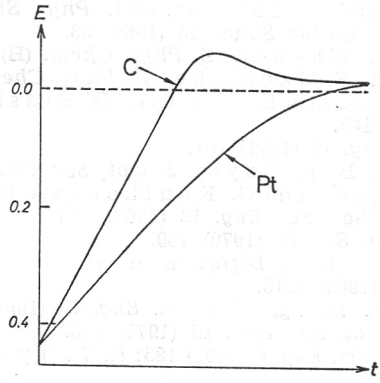

Fig. 18. Schematic potential time curves during galvanostatic pulses. Silver halide with graphite and platinum electrodes[54,55].

difference of potentials which were found with the same current density (reduction rate) at carbon and platinum contacts is a hint to the effect of latent images at the grain surface: the discrimination of exposed and unexposed grains during the development chiefly is a question of the different reaction rates at surfaces with and without nuclei.

REFERENCES

1. H. Frieser, G. Haase, and E. Klein (Editors), *Grundlagen der photographischen Prozesse,* Frankfurt/M, 1968.
2. J. N. Bradley and P. D. Greene, *Trans. Faraday Soc.* **62** (1966) 2069; **63** (1967) 424.
   B. Scrosati, G. Germano, and G. Pistoia, *J. Electrochem. Soc.* **118** (1971) 87.
3. A. B. Lidiard, *in Handbuch der Physik,* edited by S. Flügge, Vol. 20, Berlin, 1957.
4. F. A. Kröger, *J. Phys. Chem. Solids* **26** (1965) 901.
5. P. Süptitz in *Reactivity of Solids,* ed. J. W. Mitchell, *et al.* Wiley, New York, 1969, p. 29.
6. J. Teltow, *Ann. Physik* [6] **5** (1949) 71.
7. F. A. Kröger, *The Chemistry of Imperfect Crystals,* Amsterdam, 1964.
8. P. Debye, *Trans. Electrochem. Soc.* **82** (1942) 265.
9. W. Jaenicke and M. Haase, *Z. Elektrochem. Ber. Bunsenges. phys. Chem.* **63** (1959) 521;
   see K. J. Vetter, *Elektrochemische Kinetik,* Berlin—Göttingen—Heidelberg, 1961, p. 573 ff.
10. C. Wagner, unpublished (see 11).
11. N. Ibl, W. Richarz, and H. Wiederkehr, *Ind. Eng. Chem.* (1971) in press.
12. *cf* 1), p. 221.

13. C. Wagner, *Z. Elektrochem. Ber. Bunsenges. phys. Chem.* **63** (1959) 1027.
14. *cf.* 7), p. 632.
15. P. Müller, S. Spenke, and J. Teltow, *Phys. Status Solidi* **41** (1970) 81.
16. *cf.* 7), p. 210, 476.
17. M. H. Hebb, *J. Chem. Phys.* **20** (1952) 185;
C. Wagner, Proc. 7th Meeting CITCE, London 1957, p. 361.
18. F. A. Kröger, *J. Electrochem. Soc.* **117** (1970) 69.
19. R. C. Hanson, *J. Phys. Chem.* **66** (1962) 2376.
20. D. C. Burnham, F. C. Brown, and R. S. Knox, *Phys. Rev.* **119** (1960) 1560.
21. P. Süptitz, *Z. Physik* **153** (1958) 174.
22. U. Heukeroth and P. Süptitz, *Phys. Status Solidi* **13** (1966) 285; Review: J. Malinovski, *Izv. Otd. Khim. Nauk Bulg. Akad. Nauk* **2** (1970) 511.
23. W. Platikanowa and J. Malinowski, *Phys. Status Solidi* **14** (1966) 205; M. Georgiev, *Phys. Status Solidi* **15** (1966) 93.
24. H. Dünwald and C. Wagner, *Z. Phys. Chem.* (B) **24** (1943) 53.
25. E. Eisenmann and W. Jaenicke, *Z. Phys. Chem.* NF **49** (1966) 1; *Phot. Sci. Eng.* **11** (1967) 121; see also E. Schöne, O. Stasiw, and J. Teltow, *Z. Phys. Chem.* **197** (1951) 145.
26. S. Tani, *Phot. Sci. Eng.* **15** (1971) 181.
27. J. F. Hamilton and B. E. Bayer, *J. Opt. Soc. Amer.* **55** (1965) 439.
28. R. Meyer, G. Langner and G. Kaufhold, see 1) p. 1417.
29. F. Trautweiler, *Phot. Sci. Eng.* **12** (1968) 138.
30. C. R. Berry, *J. Phot. Sci.* **18** (1970) 169.
31. see 4); *Measurements of Anion Diffusion,* A. P. Batra and L. Slifkin, *J. Phys. Chem. Solids* **30** (1969) 1315.
32. E. A. Frei and W. F. Berg, *Phot Sci. Eng.* **13** (1969) 81.
33. J. Malinowski, *Phot. Sci. Eng.* **15** (1971) 175.
34. W. Jaenicke, *Phot. Sci. Eng.* **6** (1962) 185; R. W. Tyler and W. West, *Phot. Sci. Eng.* **11** (1967) 35.
35. W. Jaenicke, *J. Phot. Sci.* **20** (1972) 2.
36. R. Matejec, *Mitt. Forsch. Lab. Agfa* Vol. 4 Berlin 1968, p. 1.
37. W. Jaenicke and F. Sutter, *Z. Elektrochem. Ber. Bunsenges. phys. Chem.* **63** (1959) 722.
38. R. Matejec and E. Moisar, *Z. Elektrochem. Ber. Bunsenges. phys. Chem.* **69** (1965) 566.
39. J. D. Levine and P. Mark, *Phys. Rev.* **144** (1966) 751.
40. C. R. Berry, *Phys. Rev.* **153** (1967) 989.
41. M. I. Molotski and A. N. Catyshev, *Izv. Akad. Nauk SSSR* Ser. Fiz. **35** (1971) 359.
42. see 7), p. 773; K. L. Kliewer, *J. Phys. Chem. Solids* **27** (1966) 705, 719; L. Slifkin, W. C. McGowan, and A. Fukai, *Phot. Sci. Eng.* **11** (1967) 79.
43. T. B. Grimley and N. F. Mott, *Discussions Faraday Soc.* **1** (1947) 3; T. B. Grimley, *Proc. Roy. Soc.* (London) A **201** (1950) 40.
44. P. L. Levine, A. L. Smith, and S. Levine, *J. Colloid Interface Sci.* **34** (1970) 549.
45. see E. J. W. Verwey and J. Th. G. Overbeek, *Theory of the Stability of Hydrophobic Colloids,* New York-Amsterdam, 1948, p. 25.
46. J. F. Hamilton and L. E. Brady, *J. Appl. Phys.* **30** (1959) 1893; R. Matejec, *Phot. Sci. Eng.* **7** (1963) 123.
47. R. Matejec and R. Mayer, *Z. Phys. Chem.* NF **55** (1967) 87.
48. H. A. Hoyen and Che Yu Li, *J. Solid State Comm.* **1** (1969) 45; J. E. Hall and L. J. Bruner, *J. Chem. Phys.* **50** (1969) 1596.
49. F. Trautweiler, L. E. Brady, J. W. Castle, and J. F. Hamilton, in G. A. Somorjai (Editor) *The Structure and Chemistry of Solid Surfaces,* New York 1969; J. F. Hamilton and L. E. Brady, *Surface Sci.* **23** (1970) 389.
50. T. H. James, *Phot. Sci. Eng.* **10** (1966) 344.
51. K. Weiss, *Electrochim. Acta* **16** (1971) 201.
52. V. I. Saunders, R. W. Tyler, and W. West, *Phot. Sci. Eng.* **12** (1968) 90.
53. F. Trautweiler, *Phot. Sci. Eng.* **12** (1968) 98.
54. M. N. Hull and A. A. Pilla, *J. Electrochem. Soc.* **118** (1971) 72.
55. D. O. Raleigh, *J. Phys. Chem.* **70** (1966) 689; **71** (1967) 1785.

56. D. O. Raleigh and H. R. Crowe, *J. Electrochem. Soc.* **118** (1971) 79.
57. R. J. Friauf, *J. Chem. Phys.* **22** (1954) 1329.
58. D. Hoeschen, *Z. Phys. Chem.* NF **66** (1969) 169.
59. L. Sliwkin, see Ref. 42.
60. I. Kunze and P. Müller, *Phys. Status Solidi,* **33** (1969) 91; **38** (1970) 271.
61. K. Weiss, *Z. Phys. Chem. NF* **59** (1968) 242.
62. D. O. Raleigh, *Z. Phys. Chem.* NF **63** (1969) 319.
63. see: O. Stasiw and J. Teltow, *Abh. d. DAdW. Kl. f. Math. Phys. u. Techn.* 1960 Nr. 7. p 295; W. Rogalla and H. Schmalzried, *Ber. Bunsenges. phys. Chem.* **72** (1968) 12.
64. P. Müller, *Phys. Status Solidi* **12** (1965) 775.

IZVOD

Elektrokemijska svojstva srebrnih halogenida i njihova uloga u fotografiji

W. Jaenicke

Prikazana su svojstva AgCl, AgBr i AgJ kao ionskih vodiča, elektronskih vodiča i miješanih vodiča. Procijenjena su relaksaciona vremena točkastih dislokacija, kao i utjecaj na ravnotežu imperfekcija. Uz elektronske ravnoteže razmotreni su i Fermijevi nivoi, utjecaj okoline na nj, te pokretljivost elektrona i šupljina s osobitim obzirom na vrste zahvata u stvaranju latentne fotografske slike. Ukazuje se i na razloge visoke osjetljivosti srebrnih halogenida time, što proces fotografskog razvijanja nije redoks proces, nego površinska reakcija katalizirana niskim prenaponom na mjestu latentne slike. Porijeklo i predznak prostornog naboja u površinskom sloju diskutira se kao bitan fenomen u elektrokemijskom i fotografskom ponašanju. U opisu eksperimenata posebna je pažnja posvećena prikazivanju mjerenja polarizacije na kontaktima srebrni halogenid/metal odnosno srebrni halogenid/karbon.

INSTITUT ZA FIZIKALNU KEMIJU
UNIVERZITET ERLANGEN-NÜRNBERG
ERLANGEN, SR NJEMAČKA

Primljeno 20 siječnja 1972.